

International Journal of Modern Physics E  
 (2025) 2545006 (10 pages)  
 © World Scientific Publishing Company  
 DOI: 10.1142/S0218301325450065



[www.worldscientific.com](http://www.worldscientific.com)

## Physics-Aware POD method for cost-effective high-fidelity PGET simulations of Water-Water Energetic Reactor irradiated fuels\*

Riccardo Ferretti ††

*European Commission, Joint Research Centre,  
 Via Enrico Fermi, Ispra, I-21027, Italy*

*Politecnico di Milano, Piazza Leonardo da Vinci 32, 20133 Milano, Italy  
 riccardo.ferretti@ec.europa.eu*

Andrea Favalli<sup>†,††</sup>, Nicola Cavallini<sup>‡</sup>, Gunnar Bostrom<sup>§</sup>,  
 Aurora Fassi<sup>¶</sup>, Giovanni Mercurio<sup>||</sup> and Stefan Nonneman<sup>\*\*</sup>

*European Commission, Joint Research Centre,  
 Via Enrico Fermi, Ispra, I-21027, Italy*

<sup>†</sup>[andrea.favalli@ec.europa.eu](mailto:andrea.favalli@ec.europa.eu)

<sup>‡</sup>[nicola.cavallini@ec.europa.eu](mailto:nicola.cavallini@ec.europa.eu)

<sup>§</sup>[gunnar.bostrom@ec.europa.eu](mailto:gunnar.bostrom@ec.europa.eu)

<sup>¶</sup>[aurora.fassi@ec.europa.eu](mailto:aurora.fassi@ec.europa.eu)

<sup>||</sup>[giovanni.mercurio@ec.europa.eu](mailto:giovanni.mercurio@ec.europa.eu)

<sup>\*\*</sup>[stefan.nonneman@ec.europa.eu](mailto:stefan.nonneman@ec.europa.eu)

Stephen Croft

*Lancaster University,  
 Bailrigg, Lancaster, LA1 4YW, UK  
 s.croft@lancaster.ac.uk*

Received 14 November 2024

Accepted 24 January 2025

Published

The Passive Gamma Emission Tomography (PGET) system serves to verify spent nuclear fuel and detect pin-level diversions for international nuclear safeguards. Real measurements in the form of sinograms are necessary to test and enhance PGET performance, but they are both costly and scarce. High-fidelity Monte Carlo simulations can generate realistic data, yet they are computationally intensive, requiring all angular views (typically 360, one per degree, or even 720, one per half degree). This paper discusses how the Physics-Aware Proper Orthogonal Decomposition (PA-POD) method recently developed by our group can reconstruct a full Water–Water Energetic Reactor (VVER) sinogram from a limited number of high-fidelity angular views, significantly reducing computational costs. This paper reports on the method's

\* Based on the presentation at the International Conference on Applications of Nuclear Techniques, Crete, Greece, 18–24 June 2023.

†† Corresponding authors.

*R. Ferretti et al.*

performance, removal of the ring artifact benefits, and the procedure for constructing a comprehensive PGET library of relevant cases.

*Keywords:* Spent nuclear fuel verification; gamma tomography; limited angular views tomography; reduced order modeling; Monte Carlo simulation; nuclear safeguards; radiation imaging.

## 1. Introduction

Passive Gamma Emission Tomography (PGET) is a technique developed for verifying spent nuclear fuel and detecting diversions as part of the safeguards measures by the International Atomic Energy Agency (IAEA). The IAEA implements PGET under the Treaty on the Non-Proliferation of Nuclear Weapons (NPT) to ensure that each Member State adheres to the rules of spent nuclear fuel management and accounting. The PGET system can verify the integrity of a spent nuclear fuel assembly while it is underwater, prior to its transfer to long-term storage or a geological repository. The IAEA approved PGET for inspections in 2017.<sup>1–4</sup>

The PGET system measures the gamma-ray emissions from fission products in the fuel assembly. The most significant gamma-ray signatures come from the fission products  $^{137}\text{Cs}$ ,  $^{134}\text{Cs}$ ,  $^{154}\text{Eu}$ ,  $^{106}\text{Ru}$  and  $^{144}\text{Ce}$ , providing information about the enrichment, burnup and cooling time of the assembly.<sup>5</sup>

The analysis and interpretation of PGET measurements require comprehensive libraries covering a wide range of scenarios. Due to the cost and scarcity of experimental cases, datasets are supplemented with realistic Monte Carlo simulations.<sup>6</sup> However, these simulations entail high computational costs. As documented in the literature,<sup>6</sup> a full-fidelity transport calculation involves not only the scattering and absorption of gamma photons emitted by the fuel assembly but also those emitted due to interaction with surrounding materials, including secondary particles. This calculation includes modeling the imaging system of 182 single detectors and their responses at each angular position of a PGET scan. Furthermore, the collimation design itself results in extremely low collection efficiency, both allowed and needed in the actual measurements, due to the real photon flux being high.<sup>6</sup> All these reasons contribute to the computational expense of radiation transport Monte Carlo calculations. Studies available in the literature reported that simulating one PGET case of a fuel assembly could take about a week on a cluster with thousands of cores.<sup>6–8</sup>

The primary goal of this paper is to present an approach for creating realistic PGET libraries with significantly reduced computational cost compared to using only Monte Carlo simulations. We focus on the Water–Water Energetic Reactor (VVER) reactor fuel assembly as an example. This paper is organized as follows: first, we describe the detector system; then, we describe our method (discussed in detail in Ref. 9) and present the results of applying it to the VVER case to validate the approach. Finally, we discuss the process for creating a comprehensive PGET library for VVER and, in general, for any type of reactor fuel assembly.

*Physics-Aware POD method for cost-effective high-fidelity PGET simulations*

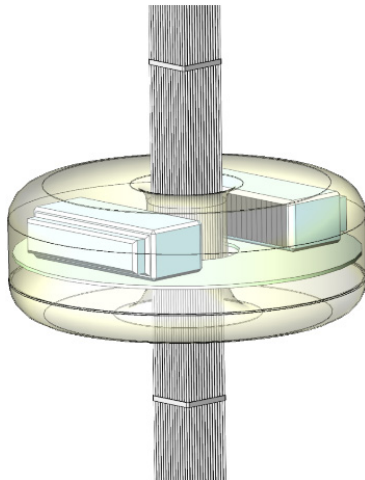


Fig. 1. 3D representation of the PGET system. The spent nuclear fuel assembly is inserted from above and then the two detection heads rotate continuously all around, collecting the gamma signal emitted by the fission products.

### 1.1. The PGET system

The PGET system consists of two arrays of 91 highly collimated CdZnTe gamma detectors mounted on a rotating plate. As depicted in Fig. 1, the components are sealed inside a metal toroid, as the system is intended to be placed inside the spent nuclear fuel pool.<sup>10</sup> The PGET measures the interaction in the detectors of the passive gamma emission of the fission products originating during reactor operation. During the measurement, the detector system rotates continuously around the fuel assembly. The measured counts vary with the angle and are grouped in energy windows. Typical values for such energy windows are < 400, 400–600, 600–700 and 700–1200 keV, while detector counts are integrated over each or half of the 360 degrees. Accordingly, the result of a measurement is a set of sinograms (an image stacking the projections of the item at different angles), one for each energy channel. The assembly's cross-sectional image showing pins distribution is then recovered by applying tomographic reconstruction algorithms.<sup>1,10,11</sup>

## 2. Methodology

### 2.1. Physics-Aware Proper Orthogonal Decomposition method

We have developed a Physics-Aware (PA) reduced-order modeling approach, in which we combine a small subset of the 360 angular views with an inexpensive solution that provides key features of the physics. This enables real-time simulations at a fraction of the cost compared to using purely a Monte Carlo approach. Among the reduced-order modeling techniques, we used Proper Orthogonal Decomposition (POD), which identifies the patterns in the data matrix through Singular Value Decomposition. We

*R. Ferretti et al.*

named this approach Physics-Aware Proper Orthogonal Decomposition (PA-POD). While the mathematical background and formulation are detailed in Ref. 9, the main steps are outlined here:

**Database creation:** Simulate only a limited set of  $N_s$  angular views and store them in a “database matrix”, namely  $\hat{S}$ . The sampling strategy, or sampled angular positions, is beyond the purpose of this work; the method holds for any possible sampling scheme.

**POD solution space creation:** Apply Singular Value Decomposition (SVD) to the database matrix. Let  $M$  be the number of CdZnTe detectors per detection head in the equation

$$\hat{S}_{M \times N_s} = U_{M \times M} \Sigma_{M \times M} V^*, \quad (1)$$

where  $U$  is the POD space matrix, signifying that its column vectors span a vector space suitable for representing an approximation of the full sinogram (i.e., the full-views sinogram). In other words, it is possible to estimate the full sinogram as a linear combination of a subset  $U_{M \times k}$  of  $k$  POD modes. Further details on the basis selection can be found in Refs. 9, 12 and 13.  $\Sigma$  is a diagonal matrix with entries as the *singular values* and  $V^*$  is the complex conjugate transpose of a unitary matrix.  $V^*$  represents the coefficients required to linearly combine the POD modes to reconstruct the database matrix. For additional details on SVD decomposition, the reader can refer to Ref. 13.

**Coefficients estimation:** Given a set of basis vectors, namely the POD modes, the problem shifts toward finding the best possible set of coefficients to linearly combine them and obtain an estimation of the full-views sinogram. This can be achieved by projecting a computationally inexpensive full-views solution into such a vector space. This inexpensive solution,  $R_{M \times 360}$ , is obtained through a fast *real-time forward approximated model* (hereafter referred to as the “real-time model”). The real-time model is a voxel model that approximates photon transport with a Lambert exponential attenuation model applied to a voxelization of the fuel assembly geometry. Further details on the implementation and assumptions of the real-time model can be found in Ref. 9. The following equation describes how this coefficient matrix is estimated:

$$C_{k \times 360} = U_{k \times M}^* R_{M \times 360}. \quad (2)$$

**Solution evaluation:** Once the coefficients of the linear combination have been estimated, it is possible to write the linear combination of POD modes representing the PA-POD estimation of the high-fidelity full-views solution for the sinogram. This denotes a more accurate solution compared to the approximation build by means of the real-time model described above. In equations:

$$S_{\text{PA-POD}} = U_{M \times k} C_{k \times 360}. \quad (3)$$

**Post-processing and ring artifact correction:** The PA-POD estimated full-views sinogram exhibits a ring artifact, indicating that the scaling across the

*Physics-Aware POD method for cost-effective high-fidelity PGET simulations*

sinogram rows can vary. According to the literature, there are several methods that can be adopted to mitigate this effect. A comprehensive review of the state-of-the-art algorithms for ring artifact correction in tomography can be found in Ref. 14. In particular, we employ the sorting technique described in Ref. 14.

## 2.2. Error quantification

Two factors contribute to favor measuring the error on the reconstructed image rather than the sinogram. First, the quality of the PGET sinogram is judged by the quality of its reconstruction.<sup>9</sup> Second, it must be considered the nonlinear mapping between the sinogram and the tomographic reconstruction (i.e., the centerline of the sinogram collapses to a pixel in the reconstruction) results in an intuitive interpretation of the error measured at a sinogram level.

For a tomographic reconstruction method, we use the analytical ramp-filtered Radon back projection, indicated here as  $\text{FBP}(\cdot)$ . The aim is to evaluate the improvement of accuracy offered by the application of the PA-POD method compared to the pure real-time model approximated solution, concerning the high-fidelity ground truth. The high-fidelity ground truth would be the ideal case of a computationally costly full-views simulation of a PGET sinogram. To give a visual idea of the error distribution, as well as a quantitative sense of its magnitude, we report the error in the form of maps of relative error with respect to a hypothetical full-views ground truth sinogram  $S_{\text{REF}}$ :

$$\text{Error map} = \left| \frac{\text{FBP}(S_{\text{PA-POD}}) - \text{FBP}(S_{\text{REF}})}{\text{FBP}(S_{\text{REF}})} \right|. \quad (4)$$

This equation is affected by divide-by-zero problems, potentially resulting in unphysical divergences of the error when the image pixel values are close to 0. To avoid this issue, we limit the calculation of the error to the assembly and its premises. The corresponding mask is obtained by selecting the only region of the image where the values are greater than 15% of the maximum.

## 3. Results: The VVER Case Study

This section presents the results of applying the PA-POD method, including the ring artifact correction, to a VVER fuel assembly type. VVER poses a significant challenge due to the strong shielding of the center of the fuel due to the other rods in the assembly. To assess the method's performance, we start with a real measured sinogram from a measured case, taken from the IAEA PGET Tomographic and Analysis Challenge (2019).<sup>15</sup> We use this data as a surrogate of realistic simulations and extract a subsample of angular views. Then, the full sonogram at each angular view is reconstructed using the recently introduced PA-POD approach.<sup>9</sup> The performance is evaluated by comparing the corresponding tomographic reconstruction (ramp-filtered back projection) with the actual measured, full-views, case (IAEA).

*R. Ferretti et al.*

$$N_s = 72, k = 72.$$

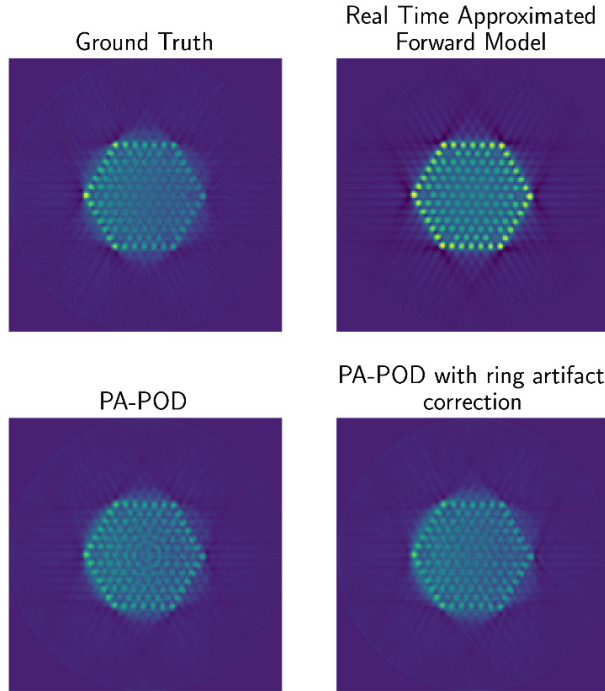


Fig. 2. VVER assembly type. Top left: filtered-back-projection of a 360-views VVER measured sinogram taken from the IAEA tomographic competition.<sup>15</sup> Top right: filtered-back-projection of a 360-views sinogram computed by means of the real-time approximated forward model, starting from a flat-intensity distribution of pins, with the specification of 6 missing pins. Bottom left: filtered-back-projection of a 360-views sinogram computed by means of the PA-POD application, starting from a set of  $N_s = 72$  out of 360 angular views, randomly chosen from the ground-truth sinogram. Bottom right: same as the bottom left, after applying ring artifact correction to the sinogram. The specific algorithms that has been chosen is the sorting technique<sup>14</sup> with a median filter size equal to 10.  $k = 72$  is the number of POD modes that are linearly combined.

Figure 2 provides an overview of the results obtained starting from a set of  $N_s = 72$  angular views, randomly chosen out from the 360 of the full-views ground truth sinogram (the approach's robustness against the random selection is further discussed in Ref. 9). The pins distribution fed to the real-time model resembles the missing pins' position but is flat (Fig. 2, top right image), while the ground truth case exhibits inhomogeneity in the activity distribution (Fig. 2, top left image), resulting in a left-to-right intensity gradient.

It is interesting to note that the PA-POD method can recover this left-to-right gradient not modeled by the real-time model, as seen in Fig. 2 (bottom left).

On the other hand, PA-POD introduces a mild ring artifact effect in the tomographic reconstruction that could potentially affect the ability to assess some of the pins.

*Physics-Aware POD method for cost-effective high-fidelity PGET simulations*

This ring effect, resulting from rows normalization inhomogeneity after applying the PA-POD method, is more severe toward the center of the assembly. The non-linearity between the sinogram and the tomographic reconstruction makes a stripe artifact at the center more visible at a tomographic reconstruction level compared to the same artifact located at the peripheral detectors. It must be pointed out that this phenomenon is common in X-ray tomography.<sup>14</sup> Usually, it is caused by the non-uniform response of the detecting system, leading to various observed stripes in the sinogram, which appear as ring artifacts in the reconstructed image. Despite many proposed methods to remove these artifacts, no single approach can be defined to remove all types of artifacts.<sup>14</sup> For our specific case, the “sorting technique” described in Ref. 14 proved to be effective. The algorithm is based on three main steps described in Ref. 14: (1) sort each column of the sinogram by its grayscale values, (2) apply a smoothing median filter of arbitrarily tuned amplitude on the sorted sinogram along each row, (3) re-sort the smoothed sinogram columns to the original position.

Figure 3 displays the maps of relative error with respect to the full-views ground truth sinogram, providing a quantitative insight into the impact of the PA-POD approach with or without ring artifact correction. Despite the real-time model not accounting for the inhomogeneity in the pins’ activity distribution, it is noteworthy that PA-POD can recover such a gradient using only 72 out of 360 angular views. Figure 3 illustrates the overall improvement in the reduction of bias in using the PA-POD with ring artifact correction.

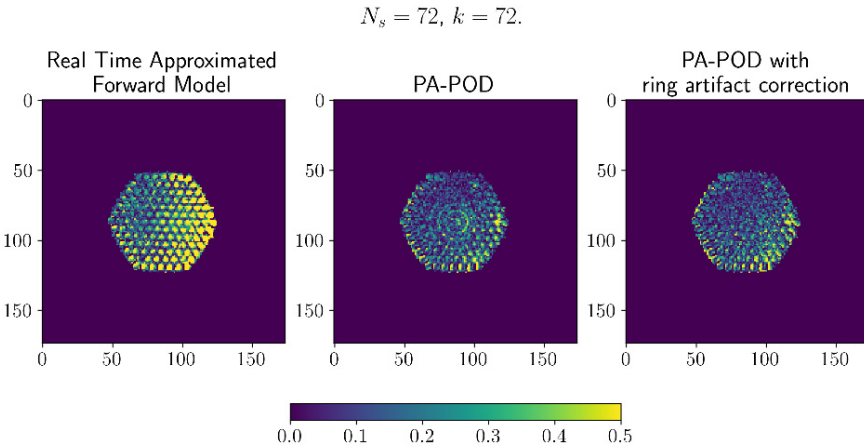


Fig. 3. Maps of relative error with respect to the tomographic reconstruction of the full-views ground truth sinogram of the VVER case included in the IAEA dataset.<sup>15</sup> The activity distribution of the pins that is fed to the real time model is flat, while the actual data exhibit an intensity gradient. The PA-POD proves to be effective in recovering such a data feature that is therefore encoded in a limited number of  $N_s = 72$  high fidelity angular views

*R. Ferretti et al.*

#### 4. PPGET Cases Library Creation

The PA-POD method with ring artifact correction demonstrates the capability to produce PGET simulations at a relatively low computational cost, enabling the construction of extended libraries. Figure 4 shows the conceptual process for constructing a library. First, relevant scenarios for a given reactor fuel assembly type (e.g., VVER) are established based on the knowledge of a subject matter expert, and the corresponding pin configurations and activity distributions are defined. These pin maps are then fed into both the real-time model and the Monte Carlo code. While the computational cost to obtain a complete 360-views from the real-time model is on the order of a few minutes on a legacy laptop,<sup>9</sup> only a limited set of angular views need to be simulated by Monte Carlo, thereby reducing the overall computational cost by a factor equal to  $N_s/360$ , where  $N_s$  is the number of simulated views. The application of the PA-POD method enables the reconstruction of all high-fidelity angular views, with an error penalty that can be balanced with respect to the number of simulated views. Reference libraries may only need to be generated once, but even so, the computational time savings of the proposed method are substantial. Additionally, the proposed method allows special investigations and sensitivity studies to be performed expeditiously on inspection cases of concern or that fall outside of expectation. From a further perspective, this framework allows the creation of a digital twin system of the PGET, a virtual model of the PGET system (e.g., AI-based) that integrates actual measurements and simulated data in continuous updates, allowing for analysis of operational measurement cases.

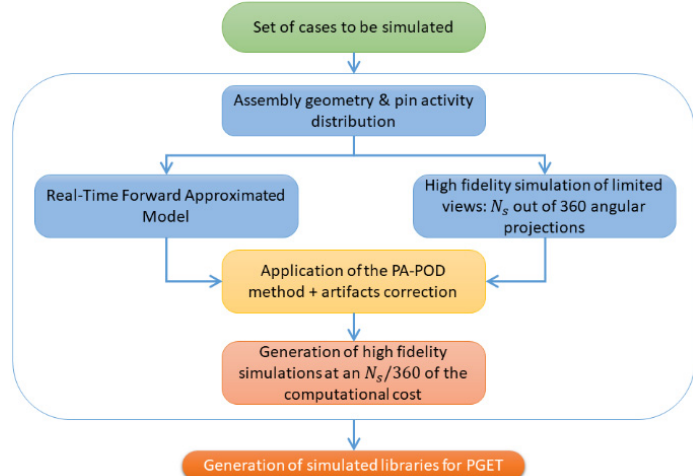


Fig. 4. Flowchart representing the conceptual framework for creating simulated libraries for the PGET.

*Physics-Aware POD method for cost-effective high-fidelity PGET simulations*

## 5. Conclusions

In this paper, we discussed the PA-POD method as an approach to reduce the computational cost of creating PGET libraries. We addressed the issue of ring artifacts originating from applying the method and discussed the mitigation of this effect in the context of relevant scientific literature. We demonstrated how proper filtering at a sinogram level can reduce the ring artifact effect and subsequently improve the accuracy of the reconstructed tomography. The process for preparing a PGET library based on the PA-POD approach has been outlined and discussed, highlighting how the development of such a library enables the evaluation of PGET applicability in a broad set of diversion scenarios, and supports the implementation and testing of novel data analysis algorithms.

## Acknowledgments

The authors warmly acknowledge the support of the Joint Research Centre of the European Commission. S.C. thanks Lancaster University for support.

## ORCID

Riccardo Ferretti  <https://orcid.org/0009-0005-3834-556X>

## References

1. M. Mayorov, T. White, A. Lebrun, J. Brutscher, J. Keubler, A. Birnbaum, V. Ivanov, T. Honkamaa, P. Peura and J. Dahlberg, Gamma emission tomography for the inspection of spent nuclear fuel, in *2017 IEEE Nuclear Science Symp. and Medical Imaging Conf. (NSS/MIC)* (IEEE, 2017), pp. 1–2.
2. A. Lebrun, J. Beaumont, A. Berlizov, L. Bourva, Y. Dodane, D. Finker, M. Mayorov and A. Sokolov, The next generation of non-destructive assay tools for IAEA safeguards verification, in *Proc. of the Symp. on Int. Safeguards* (IAEA, Vienna, 2022), pp. 1–7.
3. R. Virta, T. A. Bubba, M. Moring, S. Siltanen, T. Honkamaa and P. Dendooven, *Sci. Rep.* **12** (2022) 12473.
4. M. Fang, Y. Altmann, D. Della Latta, M. Salvatori and A. Di Fulvio, *Sci. Rep.* **11** (2021) 2442.
5. A. Favalli, D. Vo, B. Grogan, P. Jansson, H. Liljenfeldt, V. Mozin, P. Schwalbach, A. Sjöland, S. J. Tobin, H. Trellue and S. Vaccaro, *Nucl. Instrum. Methods Phys. Res. A* **820** (2016) 102.
6. L. Smith, S. Jacobsson Svärd, V. Mozin, P. Jansson, E. Miller, T. White, N. Deshmukh, H. Trellue, R. Wittman, A. Davour, S. Grape, P. Andersson, S. Vaccaro, S. Holcombe and T. Honkamaa, A Viability Study of Gamma Emission Tomography for Spent Fuel Verification: JNT 1955 Phase I Technical Report (2016).
7. E. Miller, M. Vladimir, W. Timothy, C. Luke, D. Nikhil, W. Richard and P. Pauli, Assessing instrument performance for passive gamma emission tomography of spent fuel, in *INMM 59th Annual Meeting Paper Advanced Nondestructive Assay Techniques for Fuel Assemblies* (Baltimore, Maryland, USA, 2018).
8. R. Wittman *et al.*, Benchmarking update to IAEA, Technical Report PNNL-SA-13389, Pacific Northwest National Laboratory (2018).
9. N. Cavallini, R. Ferretti, G. Bostrom *et al.*, *Sci. Rep.* **13** (2023) 15034

R. Ferretti et al.

10. C. Belanger-Champagne, P. Peura, P. Eerola, T. Honkamaa, T. White, M. Mayorov and P. Dendooven, *IEEE Trans. Nucl. Sci.* **66** (2019) 487.
11. R. Backholm, T. A. Bubba, S. Siltanen, C. Bélanger-Champagne, T. Helin and P. Den-dooven, *Inverse Probl. Imaging* **14** (2020) 317.
12. J. S. Hesthaven, G. Rozza and B. Stamm, *Certified Reduced Basis Methods for Parametrized Partial Differential Equations*, 1st edn. (Springer, 2015), p. 135.
13. S. L. Brunton and J. N. Kutz, *Data-Driven Science and Engineering: Machine Learning, Dynamical Systems, and Control*, 1st edn. (Cambridge University Press, 2019).
14. N. T. Vo, R. C. Atwood and M. Drakopoulos, *Opt. Express* **26** (2018) 28396.
15. IAEA Tomographic Challenge (2019), <https://ideas.unite.un.org/iaea-tomography/> Page/Home.